Efficient Full Waveform Inversion Subject To A Total Variation Constraint

Yudai INADA, Shingo TAKEMOTO and Shunsuke ONO
Institute of Science Tokyo

アブストラクト Full waveform inversion (FWI) aims to reconstruct subsurface properties from observed seismic data. Since FWI is an ill-posed inverse problem, appropriate regularizations or constraints are useful approaches to achieve accurate reconstruction. The total variation (TV) -type regularization or constraint is widely known as a powerful prior that models the piecewise smoothness of subsurface properties. However, the optimization problem of the TV-type regularized or constrained FWI is difficult to solve due to the non-linearity of the observation process and the non-smoothness of the TV-type regularization or constraint. Conventional approaches to solve the problem rely on an inner loop and/or approximations, resulting in high computational cost and/or inappropriate solutions. In this paper, we develop an efficient algorithm with neither an inner loop nor approximations to solve the problem based on a primal-dual splitting method. We also demonstrate the effectiveness of the proposed method through experiments using the SEG/EAGE Salt and Overthrust Models.

1 Introduction

Full waveform inversion (FWI)[1], [2] aims to reconstruct subsurface properties from observed seismic data. Since the observed seismic data are generated from the subsurface properties, FWI is formulated as an inverse problem. However, it is ill-posed, and the quality of the solution depends heavily on the initial model provided[2].

Generally, FWI reconstruct the subsurface properties by solving an optimization problem that minimizes the squared error between the observed data and the modeled data. To stabilize the inversion and achieve more accurate reconstruction, other formulations have been proposed to improve inversion results[3]–[8]. Adding regularizations or constraints to the objective function is also been proposed. Methods such as Tikhonov regularization[9], Total Variation (TV)[10], and Total Generalized Variation (TGV)[11] have been applied to FWI. For example, studies have used regularization of Tikhonov[12], TV[13], directional TV[14], high-order TV[15], and TGV as regularizations[16]. Also it have used TV as constraints[17]–[19].

Recently, neural networks (NNs) that directly estimate subsurface properties from observed data have also been proposed[20]–[23]. However, NNs require a large amount of observed data as training data, and since the dimensions of the observed data can vary depending on the observation method, training data must be prepared not only for each target but also for each observation method. Therefore, reconstruction using optimization is still useful.

Also, the value of the squared error between the observed data and the modeled data, which is the objective function of FWI, changes depending on the observation method. The parameters of the regularization need to be appropriately selected accordingly. However, with TV constraints, there is an advantage that the parameters can be determined only from prior knowledge of the subsurface properties[24].

In conventional methods that apply TV constraints to FWI[17], [18], when optimizing the usual FWI objective function using quasi-Newton methods like the L-BFGS method, the parameter updates are calculated to satisfy the constraints. Here, another optimization is required to compute the updates that satisfy the constraints, resulting in a double loop and high computational cost. Moreover, in the process of introducing constraints, approximations are used, such as treating non-linear transformations as linear or enforcing constraints outside the optimization method.

In this paper, we develop an efficient algorithm based on a primal-dual splitting method to solve the TV-constrained FWI problem without inner loops or approximations. We also demonstrate the effectiveness of the proposed method through experiments using the SEG/EAGE Salt and Overthrust Models.

2 PRELIMINARIES

2.1 Mathematical Tools

$\boldsymbol{x} \in \mathbb{R}^{\mathrm{N} \times \mathrm{M}}$ に対して L1,2 ノルムは以下のように定義されます

$$\|\boldsymbol{x}\|_{1,2} \coloneqq \sum_{\mathfrak{g} \in \mathfrak{G}} \|\boldsymbol{x}_{\mathfrak{g}}\|_2 \tag{1}$$

$\boldsymbol{x} \in \mathbb{R}^{\mathrm{N}}$ に対して TV[10] は以下のように定義されます

$$\mathrm{TV}(\boldsymbol{x}) \coloneqq \|\mathbf{D}\boldsymbol{x}\|_{1,2} = \sum_{i=1}^{\mathrm{N}} \sqrt{d_{h,i}^2 + d_{v,i}^2} \tag{2}$$

f に対する convex conjugate function は以下のように定義されます

$$f^*(\boldsymbol{y}) \coloneqq \sup_{\boldsymbol{x}} \{\boldsymbol{x}^T \boldsymbol{y} - f(\boldsymbol{x})\} \tag{3}$$

indicator function は以下のように定義されます

$$\iota_C(\boldsymbol{x}) \coloneqq \begin{cases} 0 & \text{if } \boldsymbol{x} \in C \\ \infty & \text{otherwise} \end{cases} \tag{4}$$

proximity operator は f, γ に対して以下のように定義されます

$$\mathrm{prox}_{\gamma f}(\boldsymbol{x}) \coloneqq \underset{\boldsymbol{y} \in \mathbb{R}^N}{\mathrm{argmin}} \left\{ f(\boldsymbol{y}) + \frac{1}{2\gamma}\|\boldsymbol{y} - \boldsymbol{x}\|_2^2 \right\} \tag{5}$$

indicator function に対する proximity operator は以下のように求められます.

$$\mathrm{prox}_{\gamma \iota_C(\cdot)}(\boldsymbol{x}) = P_C(\boldsymbol{x}) \coloneqq \underset{\boldsymbol{y} \in C}{\mathrm{argmin}} \|\boldsymbol{y} - \boldsymbol{x}\|_2 \tag{6}$$

box constraint に対する proximity operator は以下のように求められます.

$$P_{[a,b]^N}(\boldsymbol{x}) = \min(\max(\boldsymbol{x}, a), b) \tag{7}$$

凸共役関数に対する proximity operator は以下のように求められます [25, Theorem 3.1 (ii)].

$$\mathrm{prox}_{\gamma f^*}(\boldsymbol{x}) = \boldsymbol{x} - \gamma \mathrm{prox}_{f/\gamma}(\boldsymbol{x}/\gamma) \tag{8}$$

L1 ノルムの上界制約に対する proximity operator は以下のように求められます [26](より高速なアルゴリズムも提案されています [27]).

$$P_{\{\boldsymbol{a} \mid \|\boldsymbol{a}\|_1 \le \alpha\}}(\boldsymbol{x}) = \mathrm{SoftThrethold}(\boldsymbol{x}, \beta) \tag{9}$$

where

$$\boldsymbol{x}_{\mathrm{abs}} = \mathrm{abs}(\boldsymbol{x})$$
$$\boldsymbol{y} = \mathrm{sort}_{\mathrm{desc}}(\boldsymbol{x}_{\mathrm{abs}})$$
$$\beta' = \max\{\frac{1}{i}((\sum_{j=1}^{i} \boldsymbol{y}_j) - \alpha) \mid i = 1, \ldots, N\}$$
$$\beta = \max\{\beta', 0\}$$

L12 ノルムの上界制約に対する proximity operator は以下のように求められます [28].

$$P_{\{\boldsymbol{a} \mid \|\boldsymbol{a}\|_{1,2} \le \alpha\}}(\boldsymbol{x}) = [\boldsymbol{p}_1^T, \ldots, \boldsymbol{p}_N^T]^T \tag{10}$$

where

$$\boldsymbol{p}_i = \begin{cases} 0 & \text{if } \|\boldsymbol{x}_i\|_2 = 0 \\ \boldsymbol{\beta}_i \frac{\boldsymbol{x}_i}{\|\boldsymbol{x}\|_2} & \text{otherwise} \end{cases}$$
$$\boldsymbol{\beta} = P_{\{\boldsymbol{a} \mid \|\boldsymbol{a}\|_1 \le \alpha\}}([\|\boldsymbol{x}_1^T\|_2, \ldots, \|\boldsymbol{x}_N^T\|_2])$$

2.2 Primal-Dual Splitting Algorithm

Primal-Dual Splitting Algorithm[29]–[32] は以下の問題に対して適用されます

$$\min_{\boldsymbol{x} \in \mathbb{R}^N} \{f(\boldsymbol{x}) + g(\boldsymbol{x}) + h(\boldsymbol{L}\boldsymbol{x})\} \tag{11}$$

PDS では、以下の更新を反復的に行うことで解を求めます

$$\boldsymbol{x}^{(k+1)} = \mathrm{prox}_{\gamma_1 g}(\boldsymbol{x}^{(k)} - \gamma_1(\nabla f(\boldsymbol{x}^{(k)}) + \boldsymbol{L}^T \boldsymbol{y}^{(k)})) \tag{12}$$

$$\boldsymbol{y}^{(k+1)} = \mathrm{prox}_{\gamma_2 h^*}(\boldsymbol{y}^{(k)} + \gamma_2 \boldsymbol{L}(2\boldsymbol{x}^{(k+1)} - \boldsymbol{x}^{(k)})) \tag{13}$$

2.3 Full Waveform Inversion

FWI の目的関数以下のように定義されます

$$E(\boldsymbol{m}) = \frac{1}{2}\|\boldsymbol{u}_{\mathrm{obs}} - \boldsymbol{u}_{\mathrm{cal}(\boldsymbol{m})}\|_2^2 \tag{14}$$

ここで、$\boldsymbol{u}_{\mathrm{obs}}$ は観測された地震データ、$\boldsymbol{u}_{\mathrm{cal}(\boldsymbol{m})}$ は速度モデル $\boldsymbol{m}$ に対する計算された地震データです。また、FWI の勾配は adjoint state method を用いて計算可能です [33].

3 Proposed Method

制約付き FWI の目的関数を、PDS を用いて求解します TV 制約, box 制約付き FWI は以下の式で表されます

$$E(\boldsymbol{m}) \quad \text{s.t.} \ \ \mathrm{TV}(\boldsymbol{m}) \le \alpha \ , \ \boldsymbol{m}_{i,j} \in [a,b]^N \tag{15}$$

PDS を適用するために、制約を indicator function として目的関数に組み込みます

$$E(\boldsymbol{m}) + \iota_{\|\cdot\|_{1,2} \le \alpha}(\mathbf{D}\boldsymbol{m}) + \iota_{[a,b]^N}(\boldsymbol{m}) \tag{16}$$

PDS を適用し、得られた step は以下の通りとなります

$$\widetilde{\boldsymbol{m}}^{(k+1)} = \boldsymbol{m}^{(k)} - \gamma_1(\nabla E(\boldsymbol{m}^{(k)}) + \boldsymbol{D}^T \boldsymbol{y}^{(k)})$$
$$\boldsymbol{m}^{(k+1)} = P_{[a,b]^N}(\widetilde{\boldsymbol{m}}^{(k+1)})$$
$$\widetilde{\boldsymbol{y}}^{(k+1)} = \boldsymbol{y}^{(k)} + \gamma_2 \boldsymbol{D}(2\boldsymbol{m}^{(k+1)} - \boldsymbol{m}^{(k)})$$
$$\boldsymbol{x}^{(k+1)} = \widetilde{\boldsymbol{y}}^{(k+1)} - \gamma_2 P_{\{\boldsymbol{a} \mid \|\boldsymbol{a}\|_{1,2} \le \alpha\}}(\frac{1}{\gamma_2}\widetilde{\boldsymbol{y}}^{(k+1)})$$

ここで、$P_{[a,b]^N}(\cdot)$, $P_{\{\boldsymbol{a} \mid \|\boldsymbol{a}\|_{1,2} \le \alpha\}}(\cdot)$ はそれぞれ (7),(10) により計算可能です.

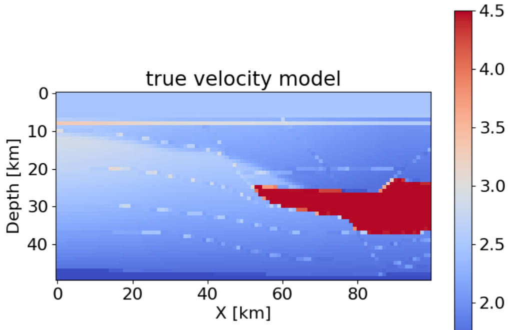

図 1: true

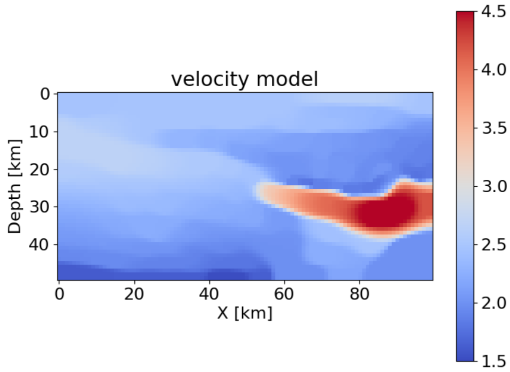

図 4: pds

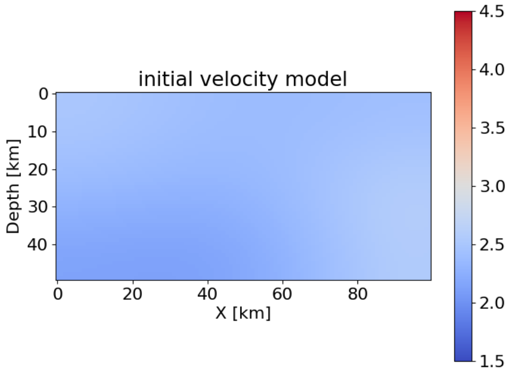

図 2: initial

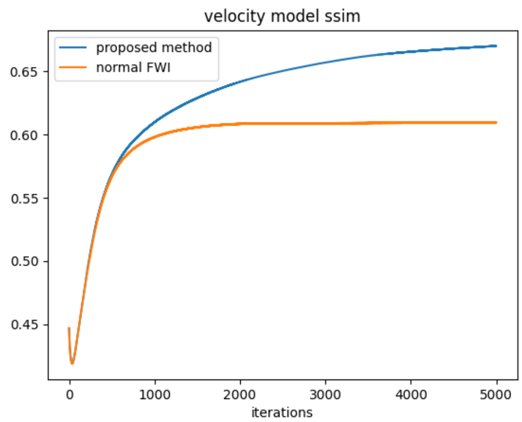

図 5: ssim

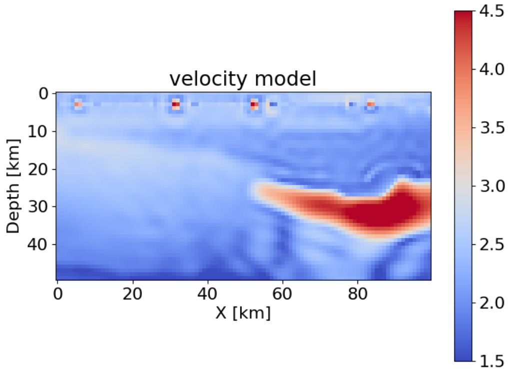

図 3: gradient

4 EXPERIMENTS

the SEG/EAGE Salt and Overthrust Models を用いて実験を行います.

参考文献

[1] A. Tarantola, "Inversion of seismic reflection data in the acoustic approximation," *Geophysics*, vol. 49, no. 8, pp. 1259–1266, 1984.

[2] J. Virieux and S. Operto, "An overview of full-waveform inversion in exploration geophysics," *Geophysics*, vol. 74, no. 6, pp. WCC1–WCC26, 2009.

[3] C. Shin and D.-J. Min, "Waveform inversion using a logarithmic wavefield," *Geophysics*, vol. 71, no. 3, pp. R31–R42, 2006.

[4] E. Bozdağ, J. Trampert, and J. Tromp, "Misfit functions for full waveform inversion based on instantaneous phase and envelope measurements," *Geophysical Journal International*, vol. 185, no. 2, pp. 845–870, 2011.

[5] J. Luo and R.-S. Wu, "Seismic envelope inversion: reduction of local minima and noise resistance," *Geophysical Prospecting*, vol. 63, no. 3, pp. 597–614, 2015.

[6] B. Engquist and B. D. Froese, "Application of the wasserstein metric to seismic signals," *arXiv preprint arXiv:1311.4581*, 2013.

[7] L. Métivier, R. Brossier, Q. Mérigot, E. Oudet, and J. Virieux, "Measuring the misfit between seismograms using an optimal transport distance: Application to full waveform inversion," *Geophysical Supplements to the Monthly Notices of the Royal Astronomical Society*, vol. 205, no. 1, pp. 345–377, 2016.

[8] M. Warner and L. Guasch, "Adaptive waveform inversion: Theory," *Geophysics*, vol. 81, no. 6, pp. R429–R445, 2016.

[9] A.-i. N. Tikhonov, A. V. Goncharsky, V. V. Stepanov, A. G. Yagola, A. Tikhonov, A. Goncharsky, V. Stepanov, and A. Yagola, *Numerical methods for the approximate solution of ill-posed problems on compact sets*. Springer, 1995.

[10] L. I. Rudin, S. Osher, and E. Fatemi, "Nonlinear total variation based noise removal algorithms," *Physica D: nonlinear phenomena*, vol. 60, no. 1-4, pp. 259–268, 1992.

[11] K. Bredies, K. Kunisch, and T. Pock, "Total generalized variation," *SIAM Journal on Imaging Sciences*, vol. 3, no. 3, pp. 492–526, 2010.

[12] A. Asnaashari, R. Brossier, S. Garambois, F. Audebert, P. Thore, and J. Virieux, "Regularized seismic full waveform inversion with prior model information," *Geophysics*, vol. 78, no. 2, pp. R25–R36, 2013.

[13] A. Y. Anagaw and M. D. Sacchi, "Full waveform inversion with total variation regularization," in *Recovery-CSPG CSEG CWLS Convention*, 2011, pp. 1–4.

[14] S. Qu, E. Verschuur, and Y. Chen, "Full-waveform inversion and joint migration inversion with an automatic directional total variation constraint," *Geophysics*, vol. 84, no. 2, pp. R175–R183, 2019.

[15] Z. Du, D. Liu, G. Wu, J. Cai, X. Yu, and G. Hu, "A high-order total-variation regularisation method for full-waveform inversion," *Journal of Geophysics and Engineering*, vol. 18, no. 2, pp. 241–252, 2021.

[16] K. Gao and L. Huang, "Acoustic-and elastic-waveform inversion with total generalized p-variation regularization," *Geophysical Journal International*, vol. 218, no. 2, pp. 933–957, 2019.

[17] E. Esser, L. Guasch, T. van Leeuwen, A. Y. Aravkin, and F. J. Herrmann, "Total variation regularization strategies in full-waveform inversion," *SIAM Journal on Imaging Sciences*, vol. 11, no. 1, pp. 376–406, 2018.

[18] E. Esser, L. Guasch, F. J. Herrmann, and M. Warner, "Constrained waveform inversion for automatic salt flooding," *The Leading Edge*, vol. 35, no. 3, pp. 235–239, 2016.

[19] P. Yong, W. Liao, J. Huang, and Z. Li, "Total variation regularization for seismic waveform inversion using an adaptive primal dual hybrid gradient method," *Inverse Problems*, vol. 34, no. 4, p. 045006, 2018.

[20] Y. Wu and Y. Lin, "Inversionnet: An efficient and accurate data-driven full waveform inversion," *IEEE Transactions on Computational Imaging*, vol. 6, pp. 419–433, 2019.

[21] S. Li, B. Liu, Y. Ren, Y. Chen, S. Yang, Y. Wang, and P. Jiang, "Deep-learning inversion of seismic data," *arXiv preprint arXiv:1901.07733*, 2019.

[22] F. Yang and J. Ma, "Deep-learning inversion: A next-generation seismic velocity model building method," *Geophysics*, vol. 84, no. 4, pp. R583–R599, 2019.

[23] V. Kazei, O. Ovcharenko, P. Plotnitskii, D. Peter, X. Zhang, and T. Alkhalifah, "Mapping full seismic waveforms to vertical velocity profiles by deep learning," *Geophysics*, vol. 86, no. 5, pp. R711–R721, 2021.

[24] B. Peters and F. J. Herrmann, "Constraints versus penalties for edge-preserving full-waveform inversion," *The Leading Edge*, vol. 36, no. 1, pp. 94–100, 2017.

[25] P. L. Combettes and N. N. Reyes, "Moreau ' s decomposition in banach spaces," *Mathematical Programming*, vol. 139, no. 1, pp. 103–114, 2013.

[26] J. Duchi, S. Shalev-Shwartz, Y. Singer, and T. Chandra, "Efficient projections onto the l 1-ball for learning in high dimensions," in *Proceedings of the 25th international conference on Machine learning*, 2008, pp. 272–279.

[27] L. Condat, "Fast projection onto the simplex and the l 1 ball," *Mathematical Programming*, vol. 158, no. 1, pp. 575–585, 2016.

[28] G. Chierchia, N. Pustelnik, J.-C. Pesquet, and B. Pesquet-Popescu, "Epigraphical projection and proximal tools for solving constrained convex optimization problems," *Signal, Image and Video Processing*, vol. 9, pp. 1737–1749, 2015.

[29] A. Chambolle and T. Pock, "A first-order primal-dual algorithm for convex problems with applications to imaging," *Journal of mathematical imaging and vision*, vol. 40, pp. 120–145, 2011.

[30] P. L. Combettes and J.-C. Pesquet, "Primal-dual splitting algorithm for solving inclusions with mixtures of composite, lipschitzian, and parallel-sum type monotone operators," *Set-Valued and variational analysis*, vol. 20, no. 2, pp. 307–330, 2012.

[31] L. Condat, "A primal–dual splitting method for convex optimization involving lipschitzian, proximable and linear composite terms," *Journal of optimization theory and applications*, vol. 158, no. 2, pp. 460–479, 2013.

[32] B. C. Vũ, "A splitting algorithm for dual monotone inclusions involving cocoercive operators," *Advances in Computational Mathematics*, vol. 38, no. 3, pp. 667–681, 2013.

[33] R.-E. Plessix, "A review of the adjoint-state method for computing the gradient of a functional with geophysical applications," *Geophysical Journal International*, vol. 167, no. 2, pp. 495–503, 2006.